THE ASTROPHYSICAL JOURNAL, 330:672–683, 1988 July 15

X-RAY SPECTRA AND LARGE-SCALE FEATURES OF TWO STARBURST GALAXIES: NGC 253 AND M82

G. FABBIANO
Harvard-Smithsonian Center for Astrophysics
Received 1987 July 28; accepted 1988 January 8

ABSTRACT

We report the results of the spatial and spectral analysis of the *Einstein* IPC observations of NGC 253 and M82. We also use the MPC data to further constrain the spectral characteristics of M82. We find that the major axis X-ray surface brightness profile of NGC 253 is steeper than the optical profile, but follows closely the radio continuum distribution. This reinforces earlier suggestions of a close link between X-ray and radio continuum emission in spiral galaxies. Extended X-ray emission with no optical or radio counterpart is found in the northern side of this galaxy. We suggest that this emission might be due to gaseous clouds ejected from the starburst nucleus. We also find that the X-ray halo of M82 extends as far as 9′ away from the nucleus along the minor axis. The radial distribution of the X-ray surface brightness of this halo is steep and suggests a density distribution $\rho \propto r^{-2}$, typical of free flowing winds. If these nuclei, and in particular M82, can be considered representative of primordial galaxies undergoing their first burst of star formation, the present day intracluster media could be the remnants of ancient starburst winds.

The spectral properties of the nuclear regions are different from those of the surrounding emission. They are fitted with large intrinsic absorption columns and possibly lower emission temperatures. The X-ray estimates of the extinction are lower than suggested by the infrared observations of these nuclei, but we cannot exclude that this is due to the poorer angular resolution needed for the X-ray spectral analysis. The emission temperatures suggest that the emission of the newly formed massive stars and that of the shock-heated interstellar medium are responsible for most of the X-ray nuclear flux of M82 detected with the IPC. The MPC data, however, suggests the presence of a harder spectral component, which could be due to binary X-ray sources with large intrinsic absorption cutoffs.

Subject headings: galaxies: individual (NGC 253, M82) — galaxies: structure — galaxies: X-rays — radio sources: galaxies — stars: formation

I. INTRODUCTION

In this paper we present the results of the *Einstein Observatory* Imaging Proportional Counter (IPC; see Giacconi *et al.* 1979 for a description of the satellite and instruments) X-ray observations of the well-known nearby starburst galaxies NGC 253 and M82. Earlier studies of the X-ray properties of these two galaxies (Fabbiano and Trinchieri 1984; Watson, Stanger, and Griffiths 1984) were based mainly on the detailed spatial analysis of the High Resolution Imager (HRI) data. This work revealed the presence of an X-ray halo along the minor axis of M82, spatially coincident with the Hα filament region, and of a plume of X-ray emission originating from the nucleus of NGC 253 and following the southern minor axis of this galaxy. Both features suggested nuclear outflows from the starburst regions. Intense spatially extended X-ray emission was found associated with the nuclear regions themselves, and a few bright point-like sources were detected both in M82 and in the spiral arms of NGC 253. The inner disk of the latter was also found to be quite bright in X-rays.

However, no information on either low surface brightness extended emission features or on the spectral characteristics of the X-ray emission could be acquired with the HRI. Only preliminary spectral results for M82 were reported by Watson, Stanger, and Griffiths (1984), by using yet uncalibrated IPC data. Here we report the results of a full spectral analysis of the *Einstein* observations of these two galaxies, made possible by the postflight calibration of the IPC (Harnden *et al.* 1984). This analysis allows us to investigate separately the spectral properties of the nuclear regions and of the emission at larger galactocentric radii. The spectral behavior in a harder energy range is also investigated with the Monitor Proportional Counter (MPC) data. The greater instrumental sensitivity of the IPC also allows us to detect faint extended features that would be invisible to the HRI, and therefore to study in detail the large scale distribution of the X-ray surface brightness of these two galaxies. This makes possible the investigation of the X-ray halo of M82 at larger radii and allows us to search for similar features in NGC 253.

II. DATA ANALYSIS

The log of the observations used in this paper is given in Table 1. The galaxies were observed with both imaging instruments, but only the IPC observations will be discussed here (see Fabbiano and Trinchieri 1984; and Watson, Stanger, and Griffiths 1984 for a discussion of the HRI results). In Table 1 we also give a summary of the integrated fluxes and luminosities of the two galaxies, as measured by the IPC and the nonimaging MPC. The IPC count rates are all in the 0.2–3.5 keV energy band, and the MPC data are in the 1–10 keV band.

The IPC count rates of both galaxies were derived from circles of 600″ radius centered on the nuclei, since X-ray emission can be detected within these areas (see §§ II*a* and II*b*). The IPC field background was estimated from the background templates produced by the *Einstein* reduction software and subtracted following the procedure described in Fabbiano and Trinchieri (1987; see also Trinchieri, Fabbiano, and Canizares

TABLE 1

EINSTEIN IPC AND MPC X-RAY OBSERVATIONS OF NGC 253 AND M82

Galaxy	Instrument	Sequence Number	Date of Observation (1979)	Time[a] (s)	Count Rate[b] (counts s^{-1})	L_x[c] (ergs s^{-1})
NGC 253	IPC	2082	Jul 1	7763	0.21 ± 0.01	1.1×10^{40}
	MPC	2082	Jul 1	5373	$\lesssim 0.3$	...
	MPC	583	Jul 5–9	12147	0.37 ± 0.08	2.5×10^{40}
M82 (NGC 3034)	IPC	466	Apr 8–9	4450	0.60 ± 0.01	3.1×10^{40}
	MPC	466	Apr 8–9	4703	0.93 ± 0.08	...
	MPC	586	May 3–6	12378	1.07 ± 0.07	6.5×10^{40}

[a] The time is the effective live time for each observation.

[b] The IPC count rates were calculated using the background-subtracted counts in the (0.2–3.5 keV) band from circles of 600″ radii centered on the galaxies' nuclei for both NGC 253 and M82. The centers are at R.A. = $0^h45^m7^s.80$ and decl. = 25°33′43″ for NGC 253 and R.A. = $9^h51^m42^s.30$ decl. = 60°55′0″ for M82. No X-ray emission associated with the two galaxies is detectable outside these circles. The background was subtracted as described in the text. The MPC count rates are in the (1.2–10.2 keV) range.

[c] The IPC luminosities are in the (0.2–4.0 keV) range and were calculated for a thermal spectra with $kT = 5$ keV and line-of-sight absorption column $N_H = 1.3 \times 10^{20}$ cm^{-2}, and $N_H = 4.3 \times 10^{20}$ cm^{-2} for NGC 253 and M82, respectively (Stark *et al.* 1988). A multiplicative factor of 1.2 was applied to the IPC count rates to correct for mirror scattering and vignetting. Distances of 3.40 Mpc and 3.25 Mpc for NGC 253 and M82, respectively, were adopted. The MPC luminosities are in the (1.2–10.2 keV) range and were calculated for the same spectral parameters as the IPC ones.

1986). The normalization of the background template calculated by the standard reduction software was used for M82. A comparison of the radial profiles of the image and background fields of NGC 253 instead suggested that the background normalization had been slightly overestimated. This can happen in fields with complex and extended emission. The background template is normalized to the field after subtracting the detected sources and some extended low-intensity emission could be included in the normalization. In our case we found that the background template needed to be multiplied by 0.94. The new normalization was calculated by matching the radial profiles of the galaxy field and the background template in the source free annular region between 720″ and 1200″ from the field center. Although we believe that this procedure gives a more correct representation of the data, the differences in both the contour map and the radial profiles (§§ II*a* and II*b*) are well within the statistical uncertainties. Figure 1 shows the good match between the radial profiles of the NGC 253 and M82 fields and the templates used for the background subtraction.

NGC 253 was not detected with the MPC during the IPC observation, but was detected at a fairly low count rate in the MPC data collected during the longer HRI observation. We report both the upper limit and the detection in Table 1. These, however, should be taken only as indicative figures, since the MPC systematics are not yet well understood and could dominate the uncertainty for very low count rates (M. Elvis 1987, private communication). IPC and MPC count rates of M82 have been previously reported by Watson, Stanger, and Griffiths (1984). Their IPC count rate is slightly smaller than that of Table 1 (0.51 instead of 0.60), but a different definition of the source area and a less accurate background subtraction (the field background templates were not available then) could explain the difference. The discrepancy between their MPC count rate and ours is significantly larger (0.39 instead of ~ 1.) and it is mostly due to Watson, Stanger, and Griffiths reporting the count rate in a narrower spectral range (2–6 keV).

a) X-Ray Contour Maps

Figures 2 and 3 show the IPC contour maps of the two galaxies overlaid onto the optical images. To obtain the IPC maps we have used the broad-band (0.2–3.5 keV) background subtracted images to optimize the statistics. No significant differences can be seen when comparing the maps from the soft (0.2–0.8 keV) and the hard (0.8–3.5 keV) bands, except that the nuclear sources are less prominent in the soft bands. The IPC data in both maps were averaged over 8″ regions. They were smoothed with Gaussians of $\sigma = 25''$ for NGC 253 and $\sigma = 35''$ for M82. We chose a narrower smoothing function for NGC 253, because we wanted to show clearly the peaks of the X-ray surface brightness due to individual sources. The significance levels of the contours were calculated using the original (non–background-subtracted) images to evaluate the statistical noise. The outermost contours in both maps represent the 2 σ level above the average background level. The positions of the point sources detected in the HRI image of NGC 253 (Fabbiano and Trinchieri 1984) are also shown in Figure 2; they tend to coincide with peaks of the IPC surface brightness distribution. A surprising feature in the X-ray image of this galaxy is the extended low surface brightness emission visible on the NW side of the optical galactic disk. Figure 3 shows dramatically the X-ray halo of M82. The presence of a halo extending out to 3′ from the nucleus had been reported by Watson, Stanger, and Griffiths (1984) based on the analysis of the HRI observation of M82. A smoothed HRI map (Kronberg, Biermann, and Schwab 1985) suggested that this emission could extend even further. This is strikingly confirmed by the IPC map.

b) Radial Distribution of the X-ray Surface Brightness

Figures 4 and 5 show radial profiles of the X-ray surface brightness of the two galaxies. The profiles of Figures 4*a* and *b* were obtained by binning in annular sectors the background-subtracted data from four pie slices centered on the nucleus of NGC 253. The "major axis" profile was derived from the parts of the image between position angles (P.A.) 30° and 90° (NE), and 210° and 270° (SW). The "minor axis" profile was derived from the parts of the image between P.A. 120° and 180° (SE), and 300° and 360° (NW). We show the four slices independently because of the obvious azimuthal asymmetry of the image. The nuclear source is extended in the high-resolution HRI image (Fabbiano and Trinchieri 1984), but it is not resolved by the IPC. The dotted curve in Figure 4*a* approximates the IPC

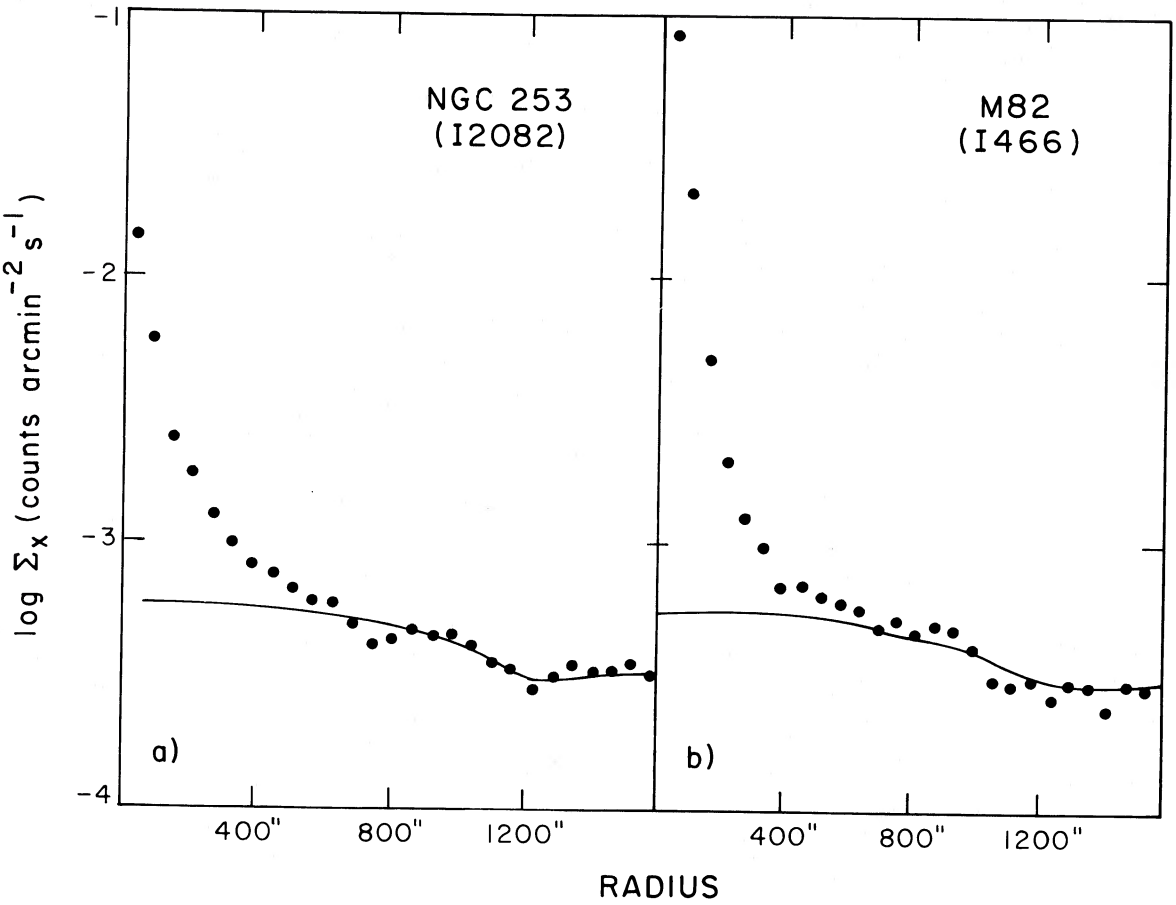

FIG. 1.—Radial distributions of the total "raw" surface brightness (*filled dots*) in the NGC 253 and M82 IPC fields, compared with the background templates (*solid lines*).

Point Response Function (PRF), and is a reasonably good fit to the centermost bins. The X-ray surface brightness can be traced out to $\sim 10'$ along the major axis. In the SE portion of the minor axis the X-ray surface brightness can be traced up to $\sim 5'$, while in the NW portion it extends to $\sim 10'$. This region corresponds to the part of the image where low surface brightness emission is visible well above the galactic plane of NGC 253.

The blue-light surface brightness profiles of Pence (1980) are sketched in Figure 4 as dashed curves. The optical major axis profile is roughly normalized to the X-ray profile in the region between 4′ and 7′ from the nucleus. The same normalization is used for the minor axis profile. The solid curves instead represent the 1.46 GHz radio continuum surface brightness profiles of Hummel, Smith, and van der Hulst (1984), obtained with a beam similar to the IPC resolution. These are normalized to the X-ray peak surface brightness. This comparison shows that (i) the X-ray emission is not detected as far as the blue light along the major axis and it follows a generally steeper radial dependence. The agreement between the X-ray and the radio surface brightness profiles is instead comparatively good. (ii) The X-ray emission clearly extends farther along the northern minor axis than either the optical or the radio emission. This extended component contributes $\sim 191.9 \pm 21.0$ net counts, which correspond to a count rate of 0.02 counts s^{-1} and a luminosity of $\sim 1.5 \times 10^{39}$ ergs s^{-1} for the parameters of Table 1. Given the IPC instrumental response, the assumption of lower temperatures $kT \approx 1$ keV will not change dramatically the estimate of the luminosity. The contour map of Figure 2 also suggests the presence of extended low surface brightness emission above the galactic plane of NGC 253 between P.A. 270° and 300°. This feature is statistically significant and contributes 70.2 ± 11.6 net counts at galactocentric radii between 4′.3 and 7′.3. The corresponding luminosity is $\sim 5.5 \times 10^{38}$ ergs s^{-1}.

The major and minor axis X-ray surface brightness profiles of M82 are shown in Figure 5. The "major axis" profile was derived from the azimuthal sectors between P.A. 0° and 90°, and 180° and 270°. The "minor axis" axis profile was derived from the complementary parts of the image. The two profiles follow each other closely in the inner 4′, and we show only the minor axis profile in the figure. The IPC PRF shown in Figure 5 was derived from the Al line (energy ≈ 1.5 keV) calibration of the IPC and mirror assembly. This IPC PRF is appropriate for the nuclear region of M82, which has a soft spectrum with $kT \approx 1.2$ keV (see below). We show the entire IPC PRF, including the mirror scattering exponential tail, and not just the Gaussian approximation, because scattered photons from the very bright nuclear component could contribute somewhat to the emission at larger radii. Figure 5 shows that the minor axis profile is more extended than the major axis one, extending as far as 9′ from the nucleus, while the latter cannot be traced past 5′. This confirms the existence of a truly diffused component of the X-ray emission, since photons scattered from

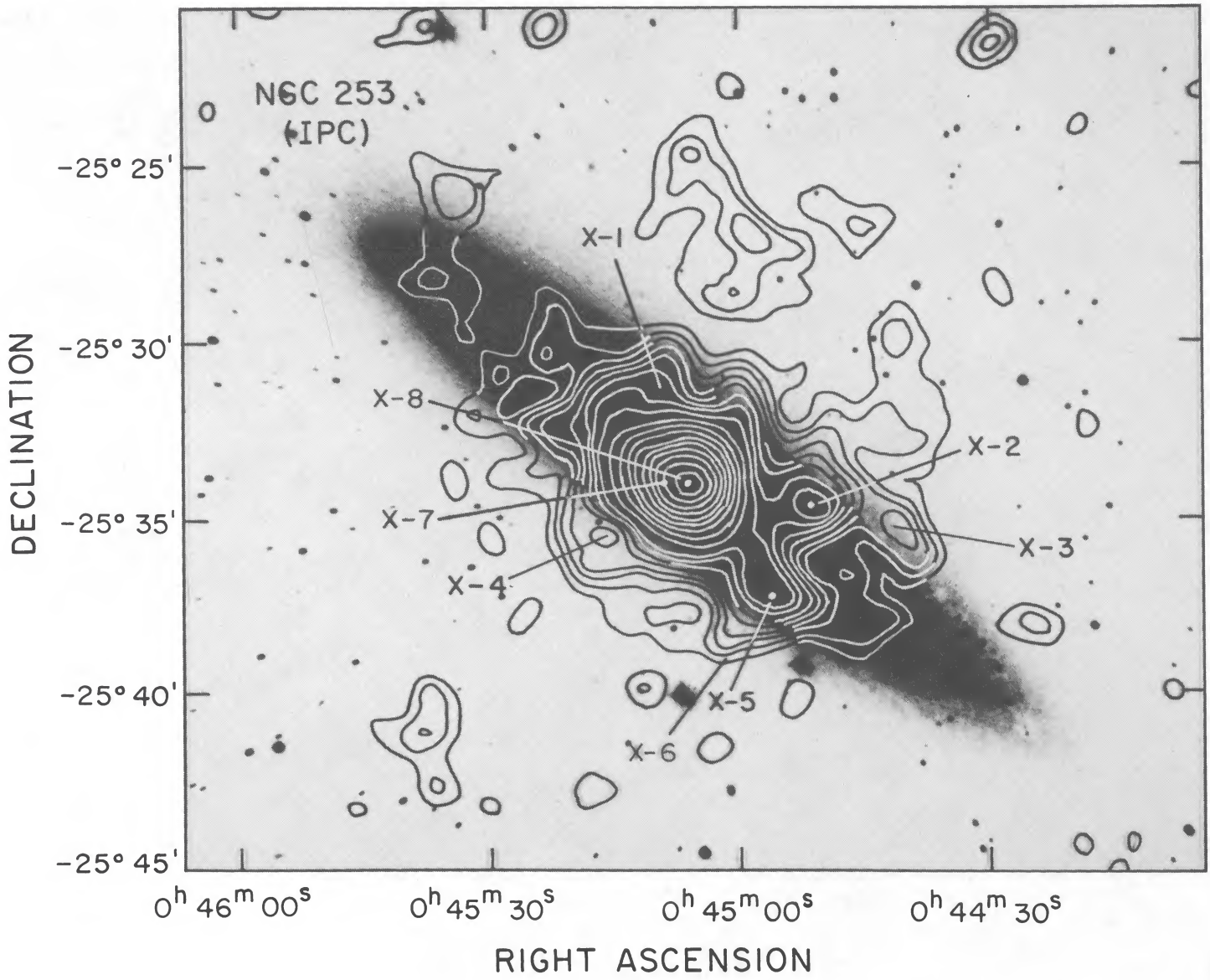

FIG. 2.—The IPC X-ray isointensity contour map of NGC 253, superposed on the POSS O plate. Data were smoothed with a Gaussian with $\sigma_G = 25''$. The first contour is at the 2 σ significance level, the next three contours follow at 1 σ intervals, and the subsequent ones are at 2 σ intervals. The IPC point response function can be approximated by a Gaussian with $\sigma \approx 45''$. The X-numbers identify the positions of the X-ray sources identified in the high-resolution HRI image of NGC 253 (Fabbiano and Trinchieri 1984).

a central point source would be distributed symmetrically. The comparison with the IPC PRF shows that the emission is also extended along the major axis of M82, between 2′ and 4′. Within the innermost 2′ the emission cannot be resolved with the IPC, but the HRI image (Watson, Stanger, and Griffiths 1984) has shown that the nuclear emission is also extended.

Using the same azimuthal sectors as for the "minor axis" profile (to which the emission from the optical body of M82 itself should not contribute), we can estimate the luminosity of the extended halo of M82. We obtain 201.4 ± 21.6 net counts between 3.′5 and 9′ from the nucleus. These translate to a count rate of 0.05 counts s^{-1} and a luminosity of $\sim 2.8 \times 10^{39}$ ergs s^{-1}, for the parameters of Table 1, (to which the emission from the optical body of M82 itself should not contribute). We estimate an uncertainty of $\sim 15\%$ on this figure, due to the photons scattered into the halo sector from the nuclear source and to the halo photons scattered out of the halo sector.

c) *Spectral Analysis*

i) *IPC*

We have performed spectral fits of the IPC data using the procedures described in Fabbiano and Trinchieri (1987). These are based on the calibrations of Harnden *et al.* (1984) and Fabricant and Gorenstein (1983). Since there is no evidence of a central nonthermal pointlike source in either NGC 253 or M82 from the HRI images (Fabbiano and Trinchieri 1984; Watson, Stanger, and Griffiths 1984), we have fitted the data of these two galaxies with an absorbed thermal spectrum (exponential plus Gaunt). We have performed spectral fits for the entire galaxies and for a series of concentric rings.

In both images the field background was estimated from the annulus between 600″ and 700″, except for the spectral fitting of the innermost regions, for which the background was also estimated from the immediately surrounding annuli. As dis-

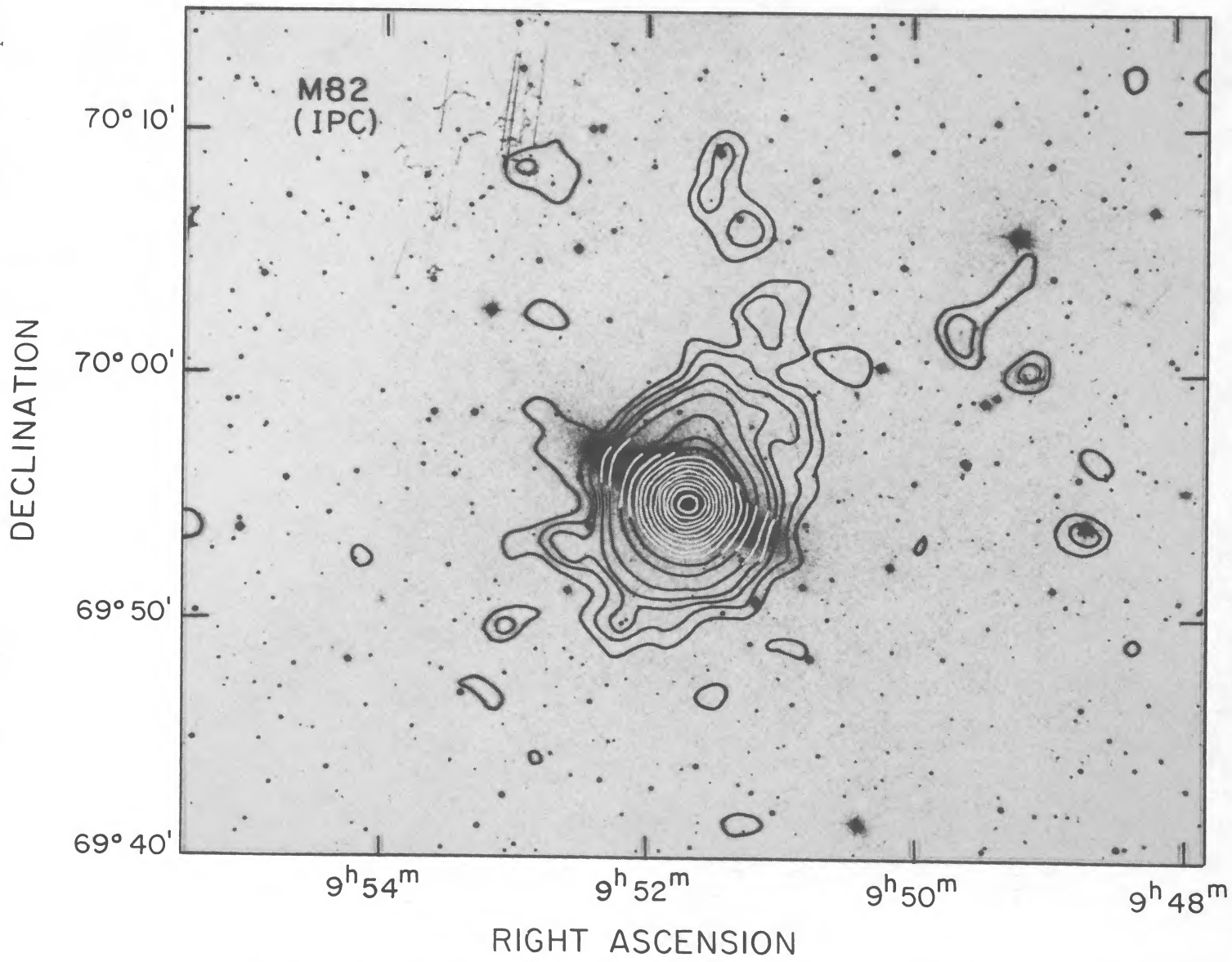

FIG. 3.—The IPC X-ray isointensity contour map of M82, superposed on the POSS O plate. The first contour is at the 2 σ level. The 3 σ; 4 σ, 5 σ, and 7 σ contours are then plotted. The subsequent contours follow at intervals of 5 σ. Data were smoothed with a Gaussian with $\sigma_G = 35''$.

cussed in Trinchieri, Fabbiano, and Canizares (1986), estimating the background from the same image used for the spectral analysis leads to smaller uncertainties than using a template field, since the spectral shape of the soft X-ray background can vary in different parts of the sky. To make sure that the radial dependence of the IPC background (see, e.g., Trinchieri, Fabbiano, and Canizares 1986) did not lead to underestimating the number of counts to be subtracted in each case, we compared the background-subtracted source counts to be used in the spectral fitting with the net counts obtained in the same region and same energy band with the "template" background subtraction. We found that in NGC 253 the background to be subtracted from the 200″ to 400″ annulus needs to be 11% higher than the one determined from the 600″ to 700″ annulus. In all the other cases the background estimate was acceptable.

The details of the spectral fitting and the results are summarized in Table 2. In both cases the data between 0.1 and 4.6 keV were included in the fit. Given the different instrumental gains of the two observations, this corresponds to fitting the data in the Pulse Height Analyser (PHA) channels 2–13 and 2–12 for NGC 253 and M82, respectively. A 3% systematic error was added in quadrature to the statistical error of each PHA channel counts, to take into account the uncertainties in the IPC calibration. The uncertainties on the spectral parameters quoted in Tables 2 and 3 are all at the 90% confidence level for two interesting parameters (Avni 1976). The confidence regions for the spectral parameters and a comparison of the best-fit model with the data are shown in Figures 6 and 7. In NGC 253 the 90% confidence contour for the entire galaxy (Fig. 6*a*) suggests equivalent temperatures $kT > 1.5$ keV and absorption columns N_H consistent with the line of sight galactic absorption of Stark *et al.* (1988; $N_H = 1.3 \times 10^{20}$ cm^{-2}), although higher absorbing columns might be preferred. A striking difference can be seen when comparing the results

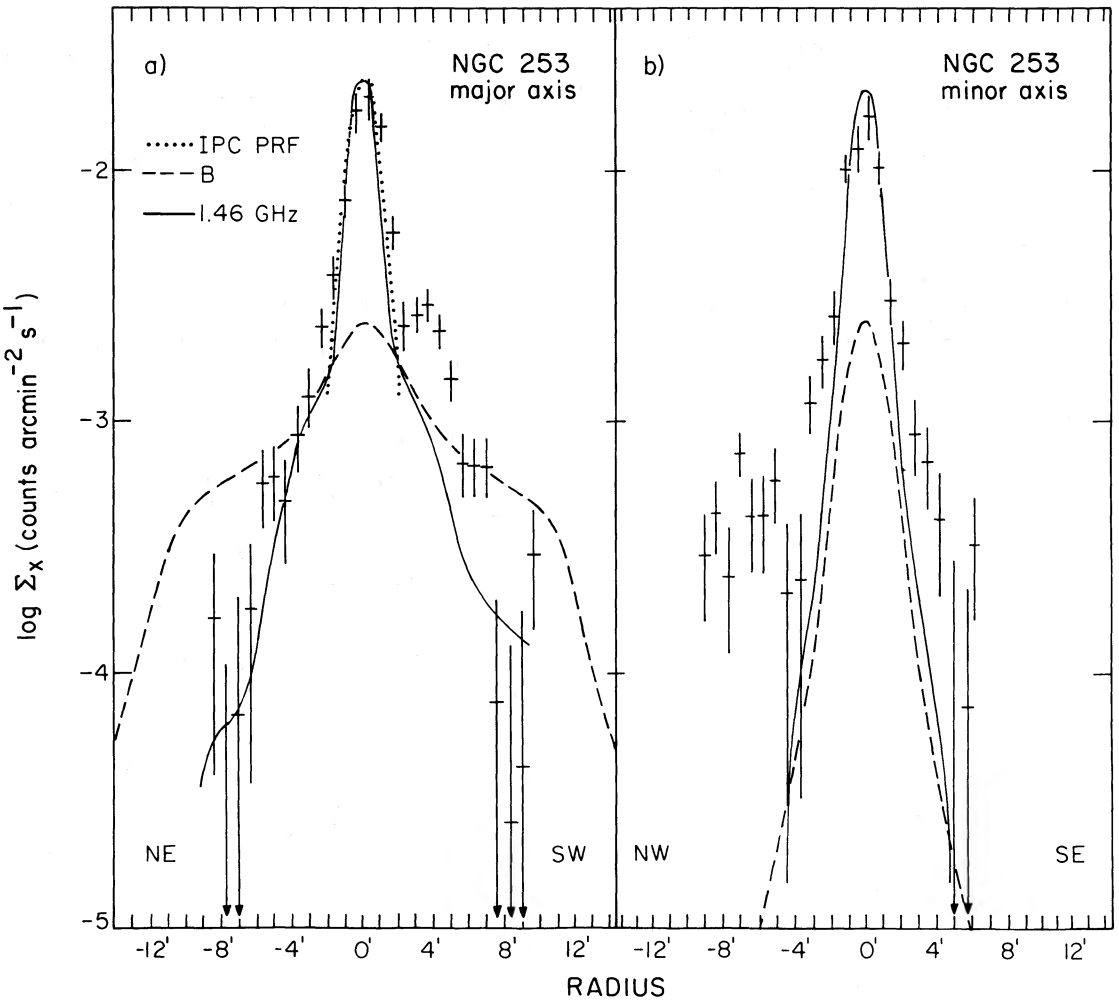

FIG. 4.—The major axis (*a*) and the minor axis (*b*) X-ray surface brightness profiles of NGC 253. The dotted curve represents the IPC point response function, the dashed lines are the B light profiles of Pence (1980), and the thin solid lines are the 1.46 GHz profiles of Hummel, Smith, and van der Hulst (1984).

TABLE 2
RESULTS OF THE SPECTRAL FITS

Source Radii	Background Radii	Total Net Counts	N_H (cm^{-2})	kT (keV)	χ^2 ν	Comments
NGC 253, IPC; R.A. = $0^h45^m7^s.80$; decl. = $-25°33'43''.0$						
0″–600″.....	600″–700″	1824.0 ± 92.7	2.0×10^{20}	5.4	7.8	The entire X-ray emission of NGC 253
			$< 8.4 \times 10^{20}$	> 1.5	9	
0–200.....	600–700	1104.5 ± 38.2	$(4.1^{+4.3}_{1.2}) \times 10^{20}$	3.3	9.8	The central/nuclear emisson.
				> 1.7	9	Only field background subtracted
0–200.....	300–400	984.8 ± 38.0	$(8.3^{+15.9}_{-4.2}) \times 10^{20}$	2.2	10.7	The central/nuclear emission.
					9	Galaxy emission subtracted.
200–400.....	600–700	479.3 ± 42.3	1.0×10^{20}	4.3	10.0	The high surface brightness nonnuclear
			$< 4.1 \times 10^{20}$	> 1.2	9	emission. The background counts were Augmented by 11% (*see text*).
M82, IPC; R.A. = $9^h51^m42^s.30$; decl. = $69°55'0''.4$						
0–600.....	600–700	2836.9 ± 81.3	$(1.7^{+1.7}_{-0.9}) \times 10^{21}$	2.2	5.8	The entire X-ray emission of M82
				> 1.2	8	
0–180.....	180–240	2160.8 ± 57.5	$(4.9^{+2.1}_{-2.5}) \times 10^{21}$	$1.2^{+1.6}_{-0.6}$	8.2	The central/nuclear emission.
					8	
200–300.....	600–700	203.8 ± 19.2	1.4×10^{20}	2.7	13.2	The nonnuclear emission.
			$< 1.2 \times 10^{21}$	> 0.6	8	

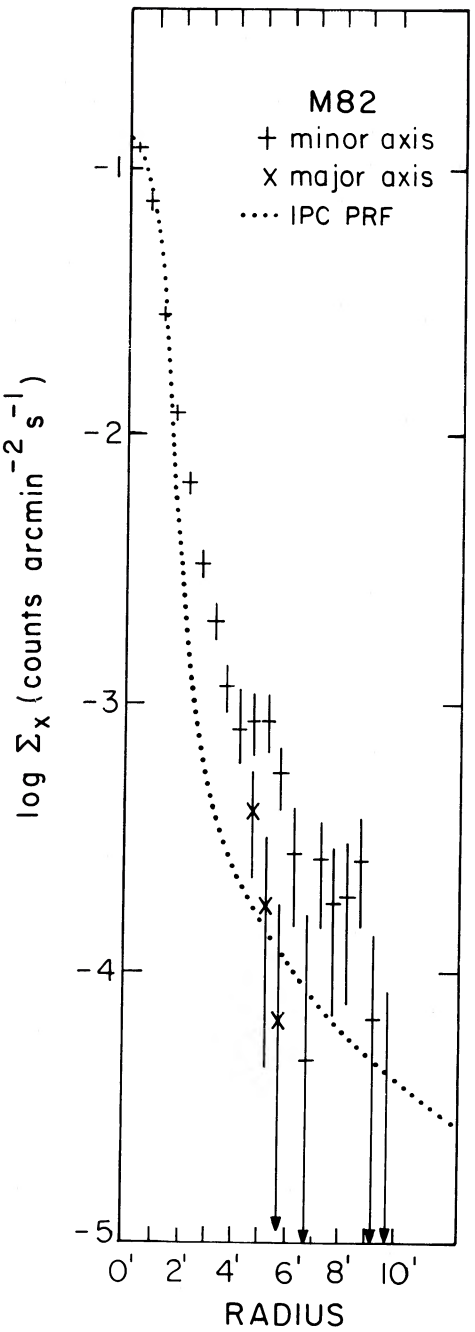

FIG. 5.—Minor- and major-axis X-ray surface brightness profiles of M82. Dotted curve represents the IPC point response function. The minor and major axis profiles follow each other closely in the inner 4′. Only the minor axis points are shown.

from the innermost nuclear region with those from the surrounding regions. While the nuclear region requires absorption columns definitely in excess of the line of sight value, the emission from the rest of the galaxy is well fitted with only the intervening galactic absorption.

The spectral fits for the nuclear region are shown in Figures 6*b* and 6*c* for two different background subtractions. Although the results do not depend strongly on the choice of the background region, higher absorption columns and possibly lower emission temperatures are suggested when the background is

TABLE 3

RESULTS OF THE SPECTRAL FIT: M82, MPC

Sequence Number	Time (s)	Total Net Counts[a]	N_H (cm^{-2})	kT (keV)	χ^2_ν
466	4703	4308 ± 396	$<6.3 \times 10^{21}$	$9.3^{+21.0}_{-5.7}$	2.9 / 3
586	12378	13256 ± 908	$<4.0 \times 10^{21}$	$5.2^{+5.2}_{-2.0}$	8.0 / 3
466 + 586[b]	17081	17564 ± 990	$<2.2 \times 10^{21}$	$6.8^{+5.7}_{-2.3}$	13.9 / 6

[a] The uncertainties on the total net counts include a systematic error to account for the uncertainties in the evaluation of the field background.

[b] This fit was done with the IoA (Cambridge) software.

estimated from the immediately surrounding annulus. This choice of background might be more realistic since it corrects for the effect of the galaxy disk emission (see Fabbiano and Trinchieri 1984), included within the central circle. The fit for the "galaxy" emission is shown in Figure 6*d*. As remarked above, the background contribution was increased by 11%, relative to the estimate from the 600″ to 700″ annulus. This correction does not produce any differences except for a small increase of the allowed parameter space, easily understandable because of the diminished signal to noise ratio.

Similar, although more extreme, results are obtained for M82 (Table 2 and Fig. 7). Fitting together the entire emission of M82, we obtain absorption columns definitely in excess of the galactic N_H of Stark *et al.* (1988) and $kT > 1.2$ keV (at the 90% confidence level; Fig. 7*a*). The data from the centermost nuclear region (Fig. 7*b*) are fitted with kT between 0.8 and 2.8 keV (at the 90%) and with an absorbing column 10 times the galactic N_H. This result does not change appreciably if the background is estimated from the 600″ to 700″ annulus, instead of from the annulus immediately surrounding the source circle, or if slightly different definitions of the source circle are used. The data from the surrounding regions do not exclude higher emission temperatures ($kT > 0.8$ keV) and are consistent with only a line of sight absorption column (Fig. 7*c*). We have also fitted the M82 data with the optically thin Raymond (J. C. Raymond, 1980, private communication) thermal spectrum, which includes the contribution of line emission. The results are in very close agreement with those reported in Table 2.

ii) *MPC Spectral Analysis of M82*

M82 was detected in the nonimaging *Einstein* MPC (Table 1; Watson, Stanger, and Griffiths 1984). The spectral information of the MPC can therefore be used to constrain further the spectral parameters of the integrated emission of M82. However, we should be careful because of the possible contamination of the MPC count rate due to the neighboring galaxy M81 (Elvis and Van Speybroeck 1982; Fabbiano 1988). The relative positions of the two galaxies are such that the MPC point response function for M81 is down to 15%–17% of the peak value (Elvis and Van Speybroeck 1982). We find that the average MPC count rate of the M81 field is ~0.7 counts s^{-1}. Therefore the contribution of M81 to the MPC count rate of the M82 field is only ~11% and will not affect significantly the spectral results.

We fitted the MPC data to the same model used for the IPC data, using only the data from the spectral channels 1–6 (1.2–10.2 keV), because the background subtraction is unreliable in

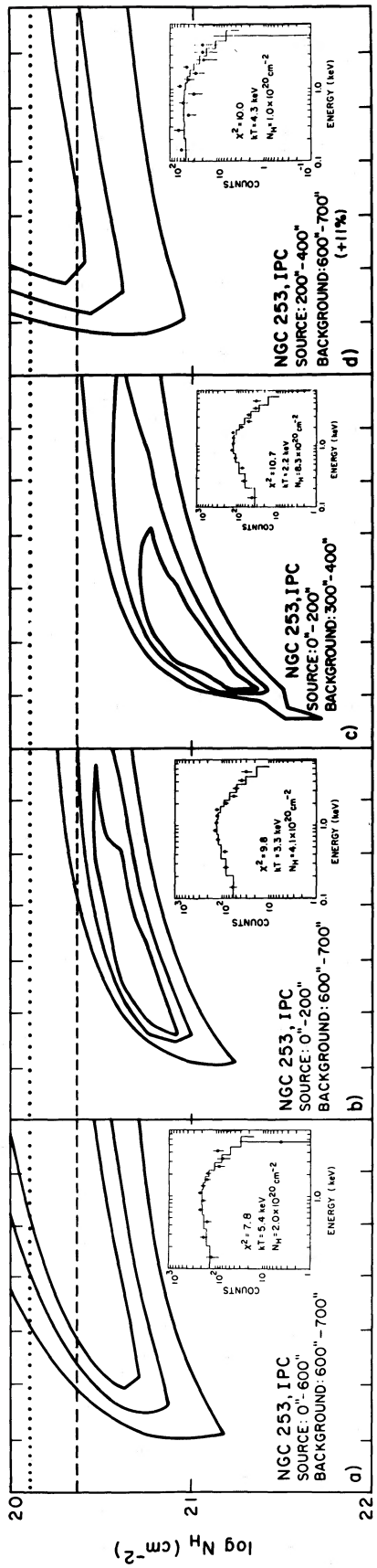

FIG. 6.—(*a–d*) The 68%, 90%, and 99% confidence contours for the spectral fits of the IPC data of NGC 253 (see text, Table 2). The dotted line represents the line of sight N_H (Stark *et al.* 1988), and the dashed line is the 90% upper bound on the line of sight N_H(see Elvis *et al.* 1986). Spectral data and the best-fit spectra are shown in the inserts.

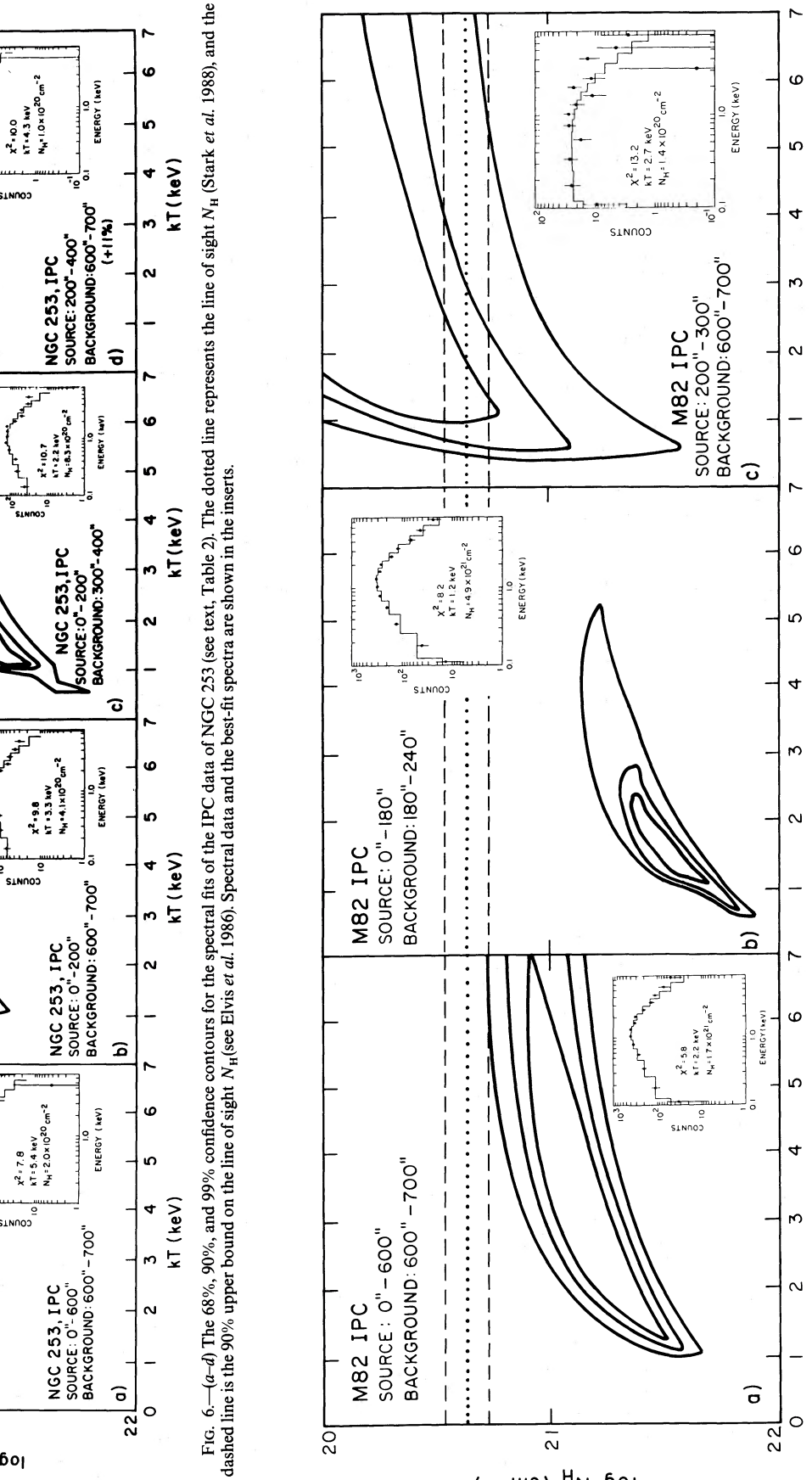

FIG. 7.—(*a–c*) The 68%, 90%, and 99% confidence contours for the spectral fits of the IPC data of M82 (see text, Table 2). The dotted line represents the line of sight N_H (Stark *et al.* 1988), and the dashed lines are the 90% bounds on this N_H(see Elvis *et al.* 1986). Spectral data and the best-fit spectra are shown in the inserts.

the higher channels. The results of the fit are given in Table 3. The MPC is sensitive at higher energies than the IPC and therefore can only determine an upper limit to the absorption column. It gives, however, a more definite constraint to the allowed temperature range, with kT between 3 and 10 keV (at 90%). These temperatures are above those allowed by the IPC spectral fitting of the nuclear region and therefore could be indicative of a complex spectrum. Similar results were obtained with the *EXOSAT* ME experiment (Schaaf *et al.* 1987).

III. DISCUSSION

a) X-Ray Halos

The *Einstein* IPC images have shown that the X-ray halo of M82 (Watson, Stanger, and Griffiths 1984) extends at least as far as 9′ from the nucleus (8.5 Kpc at a distance of 3.25 Mpc) and have revealed the presence of extended X-ray emission above the galactic plane of NGC 253, unconnected with optical or radio features. Watson, Stanger, and Griffiths discovered the X-ray halo of M82 and suggested that it is most likely due to outflowing gas heated by the energy released by supernovae in the starburst nucleus (see also Kronberg, Biemann, and Schwab 1985). This hypothesis is confirmed by the recent evidence for large-scale winds in this galaxy, given by the long-slit spectroscopic CCD observations of McCarthy, Heckman and van Breugel (1987; also J. Gallagher 1987, private communication). Unlike the symmetric X-ray halo of M82, the extended X-ray feature of NGC 253 is found only in the northern side of the galaxy. However, the lack of optical and radio counterparts and the independent evidence of nuclear outflows suggest that this feature could also be explained as thermal emission of a gaseous component. Nuclear ejection in NGC 253 was first suggested by unusual motions near the nuclear region (Demoulin and Burbidge 1970; Ulrich 1978), and has been confirmed by the presence of a plume of X-ray emission extending along the southern minor axis (seen in the high-resolution HRI data; Fabbiano and Trinchieri 1984) and by the recent CCD observations of McCarthy, Heckman and van Breugel (1987). The bipolar nature of this outflow (see Fabbiano and Trinchieri 1984) is demonstrated by the presence of a plume of OH line emission extending along the northern minor axis (Turner 1985; see also the models of Tomisaka and Ikeuchi 1987 and Chevalier and Clegg 1985). Given the inclination of NGC 253, the absence of a corresponding X-ray plume in this region can be easily understood in terms of absorption of the soft X-ray photons by the interstellar medium in the disk of NGC 253 (see Fabbiano and Trinchieri 1984). The X-ray "halo" seen in the northern side of NGC 253 could be connected with this outflow.

On the assumption that the large-scale extended features of NGC 253 and M82 are both due to gaseous haloes of temperature $T \approx 1 \times 10^7$ K, we have calculated the densities, masses, and cooling times of the X-ray emitting gas (e.g., Nulsen, Stewart, and Fabian 1984). These are given in Table 4. The main source of uncertainty in these calculations is given by the values assumed for the emitting volumes, which depend on the assumptions made about the geometrical volumes and the gas filling factors. We have assumed a truncated cone extending from 4′ to 9′ and delimited by P.A. 270° and 30° for the geometrical emission volume in NGC 253, and two truncated cones extending radially between 3.′5 and 9′ and of aperture coincident with the "minor axis" sectors in M82 (see § II*b*). In projection these would roughly correspond to the regions within which the extended features are detected. In M82 we do not include regions at radii smaller than 3.′5 to avoid contamination by the nuclear/galaxy emission. It is not clear what values of filling factors for the X-ray emitting gas one should assume. The values inferred by McCarthy, Heckman, and van Breugel for the emission line ionized gas are $\sim 1\%$. However, there are no compelling reasons to assume the same filling factors for the 10^4 K and the 10^7 K gas. Watson, Stanger, and Griffiths (1984) assumed a filling factor of 10% for the HRI X-ray halo of M82. Because of the uncertainties, the values in Table 4 are given explicitely as functions of the filling factor η. Table 4 shows that, under the above assumptions, the electron densities, masses, and cooling times of the X-ray emitting gas are: $n_e \geq 2 \times 10^3$ cm^{-3}; $M_{\rm gas} \leq 3 \times 10^7\ M_\odot$; and $\tau \leq 2 \times 10^9$ yr.

TABLE 4

HALO GAS PARAMETERS[a,b]

Galaxy	N_e (cm^{-3})	$M_{\rm gas}$ ($M_\odot$)	τ (yr)
NGC 253	$1.7 \times 10^{-3} \times 1/\sqrt{\eta}$	$2.2 \times 10^7\sqrt{\eta}$	$2.1 \times 10^9\sqrt{\eta}$
M82	$2.1 \times 10^{-3} \times 1/\sqrt{\eta}$	$3.4 \times 10^7\sqrt{\eta}$	$1.7 \times 10^9\sqrt{\eta}$

[a] See § II*b* for a description on the derivation of count rates and luminosities.

[b] The gas parameters where derived using the emissivity of Raymond, Cox, and Smith (1976) for a $\sim 10^7$ K gas; η is the gas filling factor.

What can we infer about the physical conditions of the halos, given these gas parameters and the distribution of the X-ray surface brightness? Is the gas bound to the galaxies or is it freely flowing as a wind? We will refer to M82 in the following discussion, because the evidence for the NGC 253 "halo" is rather more scanty. The more adventurous reader might like to extrapolate our conclusions to NGC 253, since similar parameters might apply.

For the gas to be expanding as a wind, in absence of gravitational confinement, its radiative cooling time must be considerably longer than the flow time (Matthews and Baker 1971). Using the expression in Matthews and Baker (1971), we estimate a wind flow time for M82 $\tau_{\rm flow} \approx 5 \times 10^7$ yr, assuming a gas temperature $T \approx 1 \times 10^7$ K. This $\tau_{\rm flow}$ would be shorter than the radiative cooling time $\tau \approx 1.7 \times 10^9\sqrt{\eta}$ yr, even for a gas filling factor $\eta \approx 1\%$, and therefore the halo is likely to be expanding freely. Supporting evidence for a free expanding wind in this galaxy is given by the radial dependence of the X-ray surface brightness profile, which at large radii can be approximated by $\Sigma_X \propto r^3$ (Fig. 8), corresponding to a radial dependence of the gas density $\rho_{\rm gas} \propto r^{-2}$ (e.g., Fabricant and Gorenstein 1983; Trinchieri, Fabbiano, and Canizares 1986), typical of free expanding winds. Following Nulsen, Stewart, and Fabian (1984), the nuclear mass-loss rate needed to sustain such a wind can be estimated as $\dot{M} \approx M_{\rm gas}/\tau_{\rm flow}$. Using our estimates of $M_{\rm gas}$ of Table 4, we find that the nuclear mass-loss rates could be as high as $\dot{M} \approx 0.7\ M_\odot$ yr^{-1}. Similar estimates are obtained by dividing the gaseous mass in the halo by the starburst time (Rieke *et al.* 1980). One must remember, however, that these estimates are likely to be upper bounds, since clumpiness in the spatial distribution of the gas would reduce them.

Figure 8 also shows that the radial dependence of the X-ray surface brightness profile of M82 within the central ~ 1.6 Kpc (100″; from the high-resolution HRI data, Watson, Stanger,

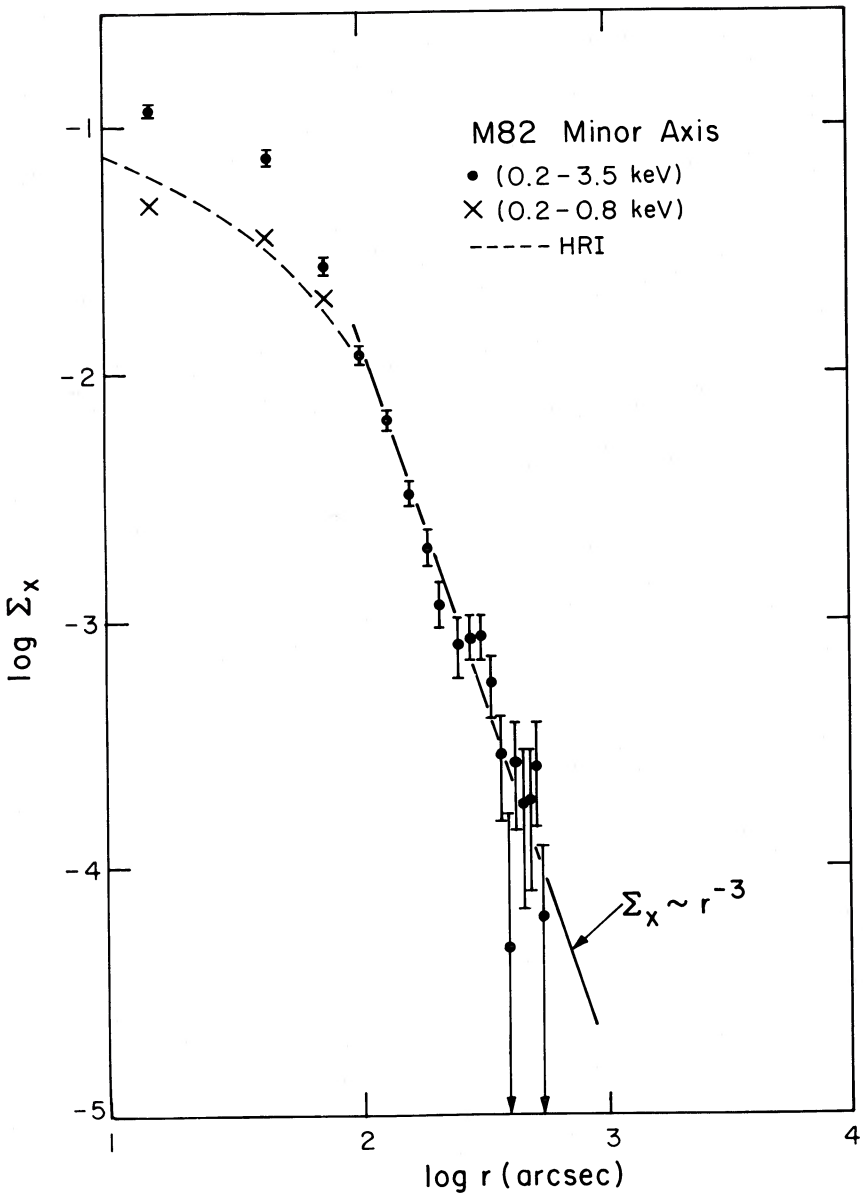

FIG. 8.—The X-ray surface brightness profile of the halo of M82 plotted in a log-log scale. The soft (0.2–0.8 keV) IPC profile and the HRI profile (Watson, Stanger, and Griffiths 1984) are both normalized to the broad-band IPC profile. The effect of the nuclear absorption is obvious from the comparison of the two IPC profiles. Notice that the similarity of the soft IPC profile and of the HRI profile is only coincidental, because at those radii the IPC distribution is mainly reflecting the IPC instrumental response (see Fig. 5). The HRI resolution instead is only a few arcseconds. At the outer radii the IPC surface brightness is well represented by a r^{-3} power law.

and Griffiths 1984) is less steep than at larger radii. Although in the centermost regions the HRI profile is likely to be depressed by absorption (see § IIc and Fig. 8), the HRI slope outside the centermost 20″ might be indicative of the intrinsic surface brightness, since these photons are emitted outside the nuclear region (e.g., Rieke *et al.* 1980). If this is indeed true, the HRI profile is reasonably fitted by the bipolar flow model of Tomisaka and Ikeuchi (1987), as noted by these authors. The steeper dependence at the outer radii, however, may suggest that the collimated expanding bubble of hot gas eventually breaks, allowing free wind expansion.

Since the halo of M82 is not likely to be radiatively confined (see above), an alternative to free wind expansion would be given by gravitational confinement. If this were the case, the X-ray data and the equation of hydrostatic equilibrium could be used to estimate the binding mass (e.g., Fabricant and Gorenstein 1983; Forman, Jones, and Tucker 1985; Trinchieri, Fabbiano, and Canizares 1986). Under these assumptions we obtain a binding mass $M = 5.4 \times 10^{11} T_7\ M_\odot$ for an isothermal gas extending to 8.5 kpc, where T_7 is the gas temperature in units of 10^7 K. The corresponding mass to light ratio is $M/L \approx 180$. These estimates are disturbingly large compared with similar estimates for bright early-type galaxies, which yield a maximum $M/L \approx 88$ (Forman, Jones, and Tucker 1985), and in any case they are rather uncertain even if gravitational confinement applies (see Trinchieri, Fabbiano, and Canizares 1986). However, there is no compelling evidence of gravitational confinement, and both the asymmetry of the halo

and the radial dependence of its X-ray surface brightness suggest that the outflow alternative is preferable. If anything, they might be considered as firm upper limits to the true values, which remain unknown.

b) Spectral Properties

The spectral analysis of the IPC data of NGC 253 and M82 has revealed the presence of absorbed X-ray emission in their starburst nuclear regions. Although significantly above the line-of-sight galactic column densities, these X-ray equivalent hydrogen column densities are, however, well below the infrared estimates. The 90% confidence upper limits on N_H of Table 2 correspond to A_V of ~ 1 and 3 mag for NGC 253 and M82, respectively (using the expression in Jenkins and Savage 1974), while the corresponding infrared values of A_V are 15 and 25 mag (Wynn-Williams *et al.* 1979; Rieke *et al.* 1980). These differences are not very surprising, because the X-ray estimates are the average values over regions of $\sim 3'$ radius, while the infrared values are relative to smaller internal regions. It is also possible, however, that the X-ray nuclear extinction is intrinsically smaller than that measured in the infrared, if the dust is distributed in the nuclear region in a nonhomogeneous fashion, as is perhaps the case in IC 342 (Fabbiano and Trinchieri 1987; Becklin *et al.* 1980) and M83 (Trinchieri, Fabbiano, and Palumbo 1985).

The X-ray emission temperatures of the nuclear regions also could differ from those of the surrounding regions. In M82, in particular, (Fig. 7) the nuclear temperatures allowed by the fit of the IPC data range between 0.8 and 2.8 keV (at the 90% confidence level), while higher temperatures could be allowed for the surrounding regions. The temperature ranges obtained for the two nuclear regions can be used to constrain the nature of their X-ray emission, because different types of X-ray sources have different characteristic temperatures.

In NGC 253 young massive binary X-ray sources, like the "Population I binary sources" of the Milky Way, are not likely to be the major component of the X-ray emission of the innermost regions, since they have a fairly hard spectral signature (with $kT > 10$ keV; e.g., Cen X-3, Schreier *et al.* 1976; 4U 0900−40 Becker *et al.* 1978; 4U 1223−62, Swank *et al.* 1976). The high-resolution HRI image of NGC 253 (Fabbiano and Trinchieri 1984; see also Fig. 2) shows that only one bright pointlike source (source No. 8) is included in the innermost region used for the spectral analysis. This region, however, includes the inner "bright disk" of this galaxy (see Fabbiano and Trinchieri 1984). By analogy with the Milky Way it is not excluded that a number of low-mass binary sources (with relatively softer X-ray spectra, typical $kT \approx 5$ keV) could contribute to its X-ray emission. Alternatively, if the inner disk is currently undergoing intense star formation (Klein *et al.* 1983; see also § III*d*), the X-ray spectrum could reflect the presence of young supernova remnants (see Gorenstein and Tucker 1976).

Tighter constraints can be put on the nature of the X-ray emission of M82. The low allowed temperatures, in fact, exclude a dominant contribution from bright binary X-ray sources to the IPC flux, in agreement with the results of Watson, Stanger, and Griffiths (1984), who find that only $\sim 25\%$ of the flux in the high-resolution HRI image is due to resolved sources. These temperatures are also rather low for the thermal emission of young supernova shells and suggest that the young massive stars in the nucleus and the extended gaseous component are responsible for the X-ray emission in the 0.2–4.5 keV range (see also Watson, Stanger, and Griffiths 1984). The higher temperatures suggested by the MPC data, however, suggest a complex, possibly two temperature spectrum [§ II*c*(ii)], and could be evidence for a contribution of massive young binary X-ray sources in a harder energy range (1.2–10 keV). These sources could have large intrinsic absorption columns and therefore not contribute much below ~ 3 keV. The possibility of an inverse Compton component in M82 is explored by Schaaf *et al.* (1987). This component would originate from the interaction of the infrared photons in the nuclear region with the relativistic electrons responsible for the radio emission.

The spectral parameters of the entire galactic emission of NGC 253, and also those of the region exterior to a 200″ radius, can be fitted with only line of sight absorption and relatively high emission temperatures, similar to those of other spiral galaxies studied in X-rays (Fabbiano and Trinchieri 1987; Trinchieri, Fabbiano, and Peres 1988). This shows that spatially resolved spectra are essential for identifying in X-rays peculiar nuclear regions in bright spiral galaxies. The spectrum of the entire X-ray emission of M82 instead, although allowing higher emission temperatures than the nuclear spectrum, is still absorbed. The spectrum of the halo is different, and it does not require intrinsic absorption: for absorbing columns consistent with the galactic absorption, emission temperatures of 1–2 keV are required to fit the data. These parameters are in agreement with our previous discussion on the gaseous halo.

c) Implications for the Intergalactic Medium and the X-Ray Background

It has been suggested that young galaxies undergoing their first massive episode of star formation can be very bright in X-rays (Bookbinder *et al.* 1980). The potential importance of winds in primordial starburst galaxies has also been recently pointed out by Heckman, Armus, and Miley (1987). It is easy to see that if the X-ray luminosity of a small starburst galaxy like M82 with an optical luminosity of $\sim 3 \times 10^9\ L_\odot$ is 3×10^{40} ergs s^{-1}, the X-ray luminosity of a primordial large elliptical system could easily be $\sim 10^{43}$ ergs s^{-1}. If the mass-loss rate from M82 is $\sim 1\ M_\odot$ yr^{-1}, a primordial galaxy might then expel $\sim 1000\ M_\odot$ yr^{-1}. Therefore, ~ 1000 such systems in a cluster, undergoing violent star formation over a period of $\sim 10^8$ yr, could produce the $\sim 10^{14}\ M_\odot$ of gas that are now found in clusters of galaxies (Jones and Forman 1984).

Weedman (1986) has suggested that the X-ray emission of starburst galaxies could be a substantial component of the X-ray background. The main unanswered question, however, is if the spectrum of the starburst X-ray emission is hard enough to be consistent with that of the X-ray background ($kT \approx 40$ keV; Marshall *et al.* 1980), or, at least, to contribute substantially to the 2 keV background, considering that most of the contribution will originate from galaxies at fairly high redshifts ($z \geq 2$). The present results, while suggesting that starburst spectra may be softer, do not exclude a contribution at energies above ~ 4 keV. It is also possible that the emission of slightly older starbursts might be entirely dominated by massive binary X-ray sources (with $kT \approx 20$ keV), and thus have a significantly harder spectrum. Although it is unlikely that starburst galaxies could contribute to the hard X-ray background, a contribution of the *Einstein* range cannot be excluded.

d) NGC 253 and the X-Ray Radio Connection in Spiral Galaxies

A strong link between radio and X-ray emission of both normal spirals and starburst galaxies was found in statistical

studies of the emission properties of these systems in different wavebands (Fabbiano, Feigelson, and Zamorani 1982; Fabbiano, Trinchieri, and Macdonald 1984; Fabbiano and Trinchieri 1985; Fabbiano, Gioia, and Trinchieri 1988) and led to the suggestion of a connection between X-ray sources and the production of cosmic rays (see also Palumbo *et al.* 1985).

The X-ray radio connection is illustrated strikingly by the similarity between the major axis X-ray surface brightness profile of NGC 253 and the radio profile of Hummel, Smith, and van der Hulst (1984). The optical profile instead follows a different, shallower, radial dependence (Fig. 4). That the nuclear source is not as prominent in the optical as in the radio and X-rays is not surprising given the large optical extinction. What is perhaps more surprising is the excess brightness of the inner disk (1′–5′) in both radio and X-ray emission relative to the optical. On the contrary, although the inner disk might be slightly brighter in X-rays, previous comparisons of surface brightness profiles in spiral galaxies have generally shown a better correspondence between the X-ray and optical distributions (in M83, Trinchieri, Fabbiano, and Palumbo 1985; M51, Palumbo *et al.* 1985; M81, Fabbiano 1988; and perhaps NGC 6946, Fabbiano and Trinchieri 1987), and in those cases in which radio continuum profiles were available (e.g., M51 and NGC 6946), the correspondence also extended to them. This excess brightness in the inner disk of NGC 253 might well be connected with continuous enhanced star formation in this region, possibly due to the presence of the bar (e.g., Klein *et al.* 1983), since enhanced star formation can result in a parallel increase of the X-ray and radio emission (Fabbiano, Trinchieri, and Macdonald 1984). An alternative explanation could be an intense past episode of star formation. This might have led to a relative increase in the population of binary X-ray sources (e.g., as in the bulge of M31, Vader *et al.* 1982), and might also be the cause of the radio excess brightness, if these X-ray sources could be directly responsible for the acceleration of cosmic-ray electrons (see Fabbiano and Trinchieri 1985).

IV. CONCLUSIONS

The extended X-ray emission found at large galactocentric radii in NGC 253 and M82 has given us new insight on both the physical conditions of the nuclear outflowing gas and on the potential importance of primordial starbursts for the formation of the intracluster medium (see also Heckman, Armus, and Miley 1987). The spectral characteristics of the X-ray emission of these two galaxies constrain the nature of the X-ray sources in the nuclear regions and show the importance of spatially resolved spectra in the X-ray study of galaxies. However, it is fair to say that we still have a long way to go toward reaching a complete understanding of the spectral properties. In particular, the possibility of complex spectra, with different temperature components, needs to be investigated further with future experiments. If it can be proven that starburst galaxies emit considerably in the harder X-rays, they could be an intriguing possibility for the origin of the soft X-ray background.

I thank Dan Weedman for pointing out the possible importance of starburst galaxies for the explanation of the X-ray background, Peter Biermann for communicating the *EXOSAT* results on M82, and Susan Gibbs for assistance in the data analysis. This work was supported under NASA contract NAS8-30751.

REFERENCES

Avni, Y. 1976, *Ap. J.*, **210**, 642.
Becker, R. H., *et al.* 1978, *Ap. J.*, **221**, 912.
Becklin, E. E., *et al.* 1980, *Ap, J.*, **236**, 441.
Bookbinder, J., Cowie, L. L., Krolik, J. H., Ostriker, J. P., and Rees, M. 1980, *Ap. J.*, **237**, 647.
Chevalier, R. A., and Clegg, A. W. 1985, *Nature*, **317**, 44.
Demoulin, M.-H., and Burbidge, E. M. 1970, *Ap. J.*, **159**, 799.
Elvis, M., Green, R. F., Bechtold, J., Schmidt, M., Neugebauer, G., Soifer, B. T., Matthews, K., and Fabbiano, G. 1986, *Ap. J.*, **310**, 291.
Elvis, M., and Van Speybroeck, L. 1982, *Ap. J. (Letters)*, **257**, L51.
Fabbiano, G. 1988, *Ap. J.*, **325**, 544.
Fabbiano, G., Feigelson, E., and Zamorani, G. 1982, *Ap. J.*, **256**, 397.
Fabbiano, G., Gioia, I. M., and Trinchieri, G. 1988, *Ap. J.*, **324**, 749.
Fabbiano, G., and Trinchieri, G. 1984, *Ap. J.*, **286**, 491.
———. 1985, *Ap. J.*, **296**, 430.
———. 1987, *Ap. J.*, **315**, 46.
Fabbiano, G., Trinchieri, G., and Macdonald, A. 1984, *Ap. J.*, **284**, 65.
Fabricant, D., and Gorenstein, P. 1983, *Ap. J.*, **267**, 535.
Forman, W., Jones, C., and Tucker, W. H. 1985, *Ap. J.*, **293**, 102.
Giacconi, R., *et al.* 1979, *Ap. J.*, **230**, 540.
Gorenstein, P., and Tucker, W. H. 1976, *Ann. Rev. Astr. Ap.*, **14**, 373.
Harnden, F. R., Fabricant, D. G., Harris, D. E., and Schwarz, J. 1984, *Scientific Specifications of the Data Analysis System for the Einstein Observatory (HEAO 2) IPC*, Internal SAO Special Report No. 393.
Heckman, T. M., Armus, L., and Miley, G. 1987, *A.J.*, **92**, 276.
Hummel, E., Smith, P., and van der Hulst, J. M. 1984, *Astr. Ap.*, **137**, 138.
Jenkins, E. B., and Savage, B. O. 1974, *Ap. J.*, **187**, 243.
Jones, C., and Forman, W. 1984, *Ap. J.*, **276**, 38.
Klein, U., Urbanik, M., Beck, R., and Wielebinski, R. 1983, *Astr. Ap.*, **127**, 177.
Kronberg, P. P., Biermann, P., and Schwab, F. R. 1985, *Ap. J.*, **246**, 751.
Marshall, F. E., Boldt, E. A., Holt, S. S., Miller, R. B., Mushotzky, R. F., Rose, L. A., Rothschild, R. E., and Serlemitsos, P. J. 1980, *Ap. J.*, **235**, 4.
Matthews, W., and Baker, J. 1971, *Ap. J.*, **170**, 241.
McCarthy, P. J., Heckman, T., and van Bruegel, W. 1987, *A.J.*, **92**, 264.
Nulsen, P. E. J., Stewart, G. C., and Fabian, A. C. 1984, *M.N.R.A.S.*, **208**, 185.
Palumbo, G. G. C., Fabbiano, G., Fransson, C., and Trinchieri, G. 1985, *Ap. J.*, **298**, 259.
Pence, W. D. 1980, *Ap. J.*, **239**, 54.
Raymond, J. C., Cox, D. P., and Smith, B. W. 1976, *Ap. J.*, **204**, 290.
Rieke, G. H., Lebofsky, M. J., Thompson, R. I., Low, F. J., and Tokunaga, A. T. 1980, *Ap. J.*, **238**, 24.
Schaaf, R., Pietsch, W., Biermann, P. L., Kronberg, P. P., and Schmutzler, T. 1987, preprint.
Schreier, E., Swartz, K., Giacconi, R., Fabbiano, G., and Morin, J. 1976, *Ap. J.*, **204**, 539.
Stark, A. A., Heiles, C., Bally, J., and Linke, R. 1988, in preparation.
Swank, J. H., *et al.* 1976, *Ap. J. (Letters)*, **209**, L57.
Tomisaka, K., and Ikeuchi, S. 1987, preprint.
Trinchieri, G., Fabbiano, G., and Canizares, C. R. 1986, *Ap. J.*, **310**, 637.
Trinchieri, G., Fabbiano, G., and Palumbo, G. G. C. 1985, *Ap. J.*, **290**, 96.
Trinchieri, G., Fabbiano, G., and Peres, G. 1988, *Ap. J.*, **325**, 531.
Turner, B. E. 1985, *Ap. J.*, **299**, 312.
Ulrich, M.-H. 1978, *Ap. J.*, **219**, 424.
Vader, J. P., van den Heuvel, E. P. J., Lewin, W. H. G., and Takens, R. J. 1982, *Astr. Ap.*, **113**; 328.
Watson, M. G., Stanger, V., and Griffiths, R. E. 1984, *Ap. J.*, **286**; 144.
Weedman, D. 1976, in "Star formation in Galaxies", NASA Conference Publication 2466, C. J. Lonsdale Persson, colour page 351, preprint.
Wynn-Williams, C. G., Becklin, E. E., Matthews, K., and Neugenbauer, C. 1979, *M.N.R.A.S.*, **189**, 163.

G. FABBIANO: Harvard-Smithsonian Center for Astrophysics, 60 Garden Street, Cambridge, MA 02138